

Parametric Study on Performance of Straight Type of Internally Finned Tube [†]

Chun-Lang Yeh ^{*}, Dong-Long Wu, Qi-Ying Cai, Yu-Xi Chung, Chang-Xin Liu and Zhi-Qian Wu

Department of Aeronautical Engineering, National Formosa University, Yunlin 632, Taiwan; 10978104@nfu.edu.tw (D.-L.W.); 11078104@nfu.edu.tw (Q.-Y.C.); 11178121@nfu.edu.tw (Y.-X.C.); 40831246@nfu.edu.tw (C.-X.L.); 40831239@nfu.edu.tw (Z.-Q.W.)

^{*} Correspondence: clyeh@nfu.edu.tw; Tel.: +886-5-6315527

[†] Presented at the 3rd IEEE International Conference on Electronic Communications, Internet of Things and Big Data Conference 2023, Taichung, Taiwan, 14–16 April 2023.

Abstract: The performance of a straight type of internally finned tube (SIFT) is studied using computational fluid dynamics (CFD). It is found that a longer fin yields a larger pressure drop that is nearly proportional to the fin length. When the fin length is larger than 30 d, the pressure drop is greater than that of a bare tube. The temperature uniformity decreases with the fin length of the SIFT. Furthermore, a smaller fin angle yields a larger pressure drop, while a larger fin angle yields better temperature uniformity. A larger contraction yields a larger pressure drop, too.

Keywords: SIFT; temperature uniformity; pressure drop; fin length; fin angle; fin amplitude

1. Introduction

Mixing in a pipe system is important in industrial applications. There are two major mixing-enhanced methods: active and passive methods. The former uses an external energy source, while the latter includes no moving parts. The passive mixing-enhanced devices increase an internal surface area and enhance the flow mixing. The solid fin and the straight type of internally finned tube (SIFT) have an increased surface area [1–5]. With enhanced flow mixing, radial mixing occurs in the tube which consequently yields a more homogeneous process. The radial mixing is found in the helical type of internally finned tube (HIFT), the mixing element radiant tube (MERT) by Kubota, the intensified heat transfer (IHT) by Lummus and Sinopec, and the SIFT technology. In Ref. [6], the HIFT was investigated numerically. In this study, the performance of the SIFT concerning heat transfer enhancement and pressure drop gain is investigated using computational fluid dynamics (CFD) to obtain better thermal uniformity and minimize pressure drop.

2. Numerical Methods

In this research, we use ANSYS FLUENT V.17 [7] to analyze the flow development in the SIFT. The SIMPLE algorithm is used for the solution algorithm [8]. In turbulence modeling, we adopt the transition shear stress transport (SST) model. Considering the accuracy and stability, we used the discrete ordinate radiation model [9] for radiation simulation.

3. Results and Discussion

In this study, the parameters include fin angle (2α), fin amplitude (in terms of radiuses R_a and R_i), and fin length (L) to obtain better thermal uniformity and minimize pressure drop. Figure 1 illustrates the investigated SIFT. The tube length is 132 d (d is a pipe diameter of 50.7 mm). Fourteen different helix lengths ranging from $L = 0$ (i.e., bare tube) to $L = 132$ d are investigated to study the influence of helix length. Three different fin angles (2α), including $2\alpha = 30^\circ$, 45° , and 60° and four different R_a , including 0.99, 0.9, 0.8, and 0.7 R_t , as



Citation: Yeh, C.-L.; Wu, D.-L.; Cai, Q.-Y.; Chung, Y.-X.; Liu, C.-X.; Wu, Z.-Q. Parametric Study on Performance of Straight Type of Internally Finned Tube. *Eng. Proc.* **2023**, *38*, 37. <https://doi.org/10.3390/engproc2023038037>

Academic Editors: Teen-Hang Meen, Hsin-Hung Lin and Cheng-Fu Yang

Published: 26 June 2023



Copyright: © 2023 by the authors. Licensee MDPI, Basel, Switzerland. This article is an open access article distributed under the terms and conditions of the Creative Commons Attribution (CC BY) license (<https://creativecommons.org/licenses/by/4.0/>).

well as four different R_i , including 0.9, 0.8, 0.7 and 0.6 R_i , where $R_t = d/2$ are used for the investigation. The boundary conditions are outlined as follows.

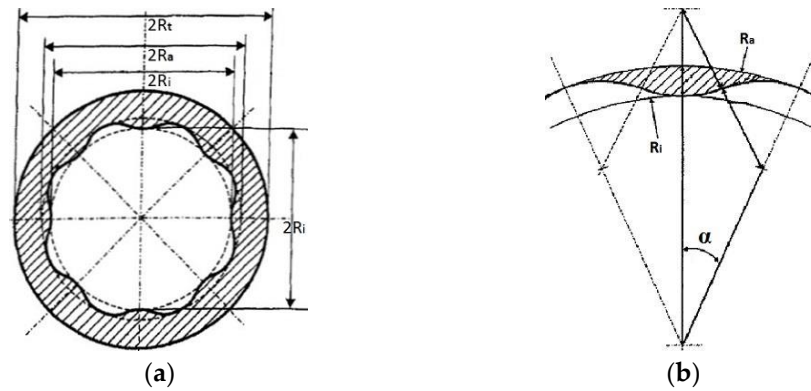


Figure 1. Illustration of the SIFT investigated: (a) cross-sectional view; (b) zoom-in view of a fin.

The tube inlet (Figure 2) includes four parts. In Region 1, $V = 56.2$ m/s and $T = 273.15$ K, in Region 2, $V = 61.3$ m/s and $T = 298.15$ K, in Region 3, $V = 66.5$ m/s and $T = 323.15$ K, and in Region 4, $V = 71.6$ m/s and $T = 348.15$ K. The inlet turbulence kinetic energy (k) is assumed to be 10% of $V^2/2$. The turbulence dissipation rate is modeled by Equation (1).

$$\epsilon = C_\mu^{3/4} \frac{k^{3/2}}{l} \tag{1}$$

In Equation (1), the constant $C_\mu = 0.09$, parameter $l = 0.07L$, and the hydraulic diameter L is equal to the pipe diameter d . At the wall boundaries, the transition SST model automatically takes the wall effects into account. Furthermore, adiabatic walls are assumed. At the tube exit, the gauge pressure is zero. The outflow diffusion flux for the other flow variables is zero, and the conservation of mass is satisfied.

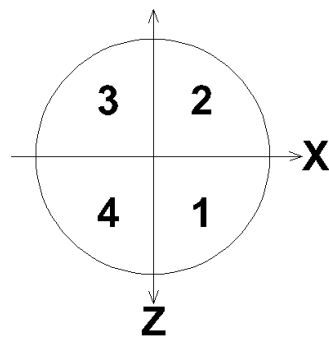


Figure 2. Division of the inlet.

The effect of fin length on the pressure variation along the tube is shown in Figure 3. The pressure drop increases with the fin length nearly in proportion. The pressure drop is closely related to the tube’s inner surface friction, which is connected to the fin length. When the fin length is larger than 30 d , the pressure drop is greater than that of a bare tube.

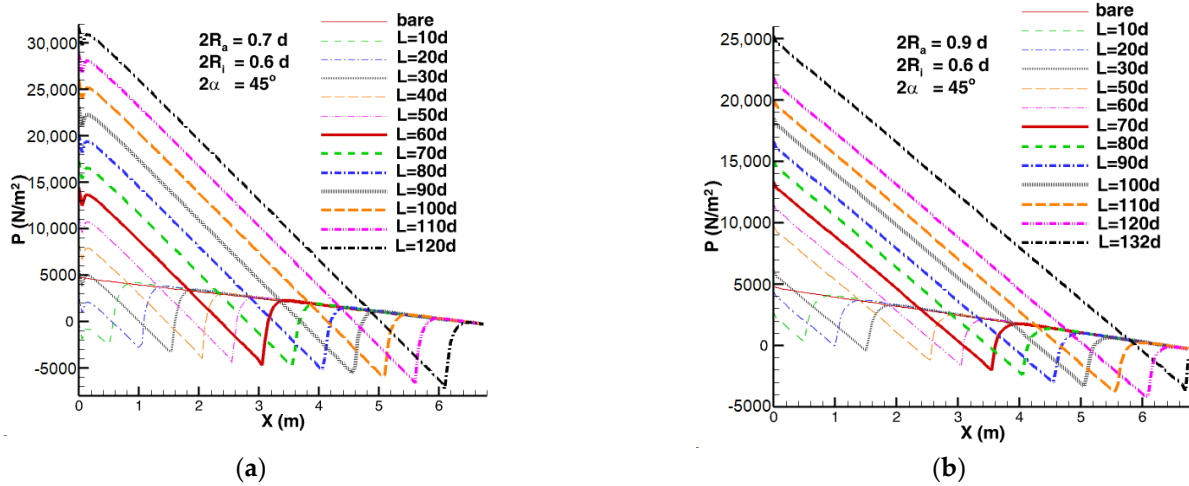


Figure 3. Variation of the cross-sectional average pressure: (a) $2R_a = 0.7d$, $2R_i = 0.6d$, $2\alpha = 45^\circ$; (b) $2R_a = 0.9d$, $2R_i = 0.6d$, $2\alpha = 45^\circ$.

The effect of fin length on the cross-sectional average temperature distribution along the tube is shown in Figure 4. The temperature of the SIFT is higher than that of a bare tube. The temperature of the SIFT rises abruptly at the fin inlet due to the contraction of the tube and descends abruptly at the fin outlet due to the expansion of the tube. In addition, the temperature becomes higher for a longer fin because the tube wall frictional heating and the flow acceleration in the fin region are larger.

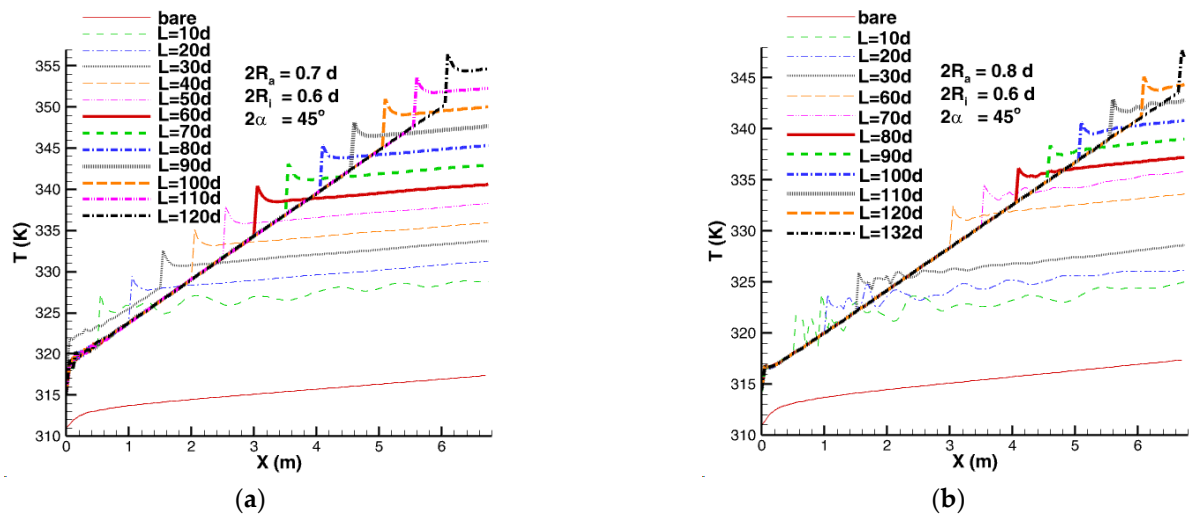


Figure 4. Variation of the cross-sectional average temperature: (a) $2R_a = 0.7d$, $2R_i = 0.6d$, $2\alpha = 45^\circ$; (b) $2R_a = 0.8d$, $2R_i = 0.6d$, $2\alpha = 45^\circ$.

The effect of fin length on the area-weighted temperature uniformity index defined as Equation (2) [7] is shown in Figure 5.

$$\gamma_a = 1 - \frac{\sum_{i=1}^n [(|T_i - \bar{T}_a|)] A_i}{2|\bar{T}_a| \sum_{i=1}^n A_i} \tag{2}$$

In Equation (2), i is the facet index and n is the number of facets of a surface. \bar{T}_a is the surface average temperature.

$$\bar{T}_a = \frac{\sum_{i=1}^n T_i A_i}{\sum_{i=1}^n A_i} \tag{3}$$

A value of one indicates optimal uniformity. Figure 5 shows that SIFT improves temperature uniformity as compared to a bare tube. The change in the temperature uniformity index is similar to fin lengths. In the fin, the temperature uniformity index for different fin lengths nearly coincides, while after leaving the fin region, the temperature uniformity increases to another coincident value for different fin lengths. Therefore, there is no need to use an SIFT with a long fin. A fin length of 10 d is enough to obtain satisfactory temperature uniformity.

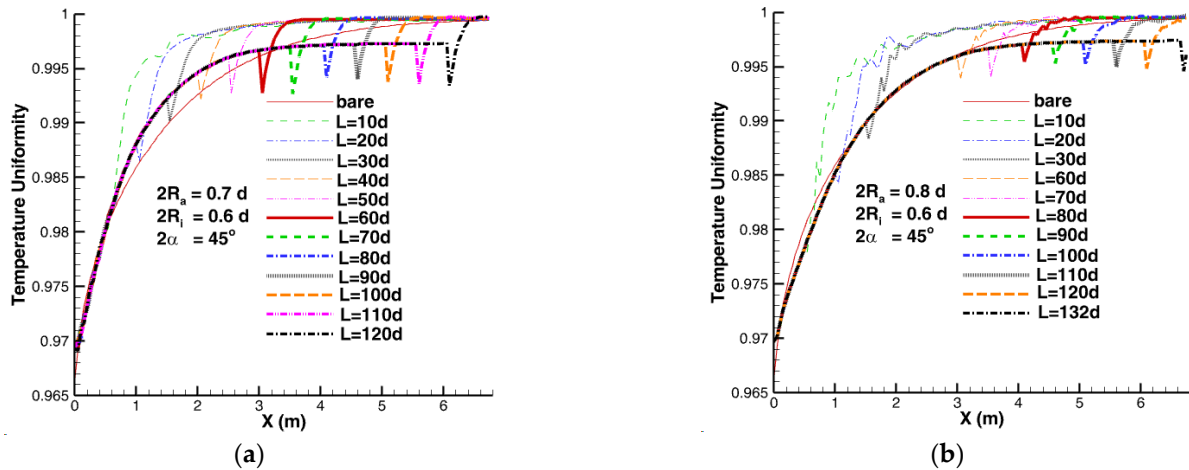


Figure 5. Temperature uniformity index along the tube: (a) $2Ra = 0.7d$, $2Ri = 0.6d$, $2\alpha = 45^\circ$; (b) $2Ra = 0.8d$, $2Ri = 0.6d$, $2\alpha = 45^\circ$.

The effect of the fin angle on the pressure variation along the tube is shown in Figure 6. A smaller fin angle yields a larger pressure drop. The pressure drop is closely related to the tube’s inner surface friction. Because the wall area is connected to the fin, a smaller fin angle corresponds to more fins, which in turn have a larger inner surface area and larger pressure drop.

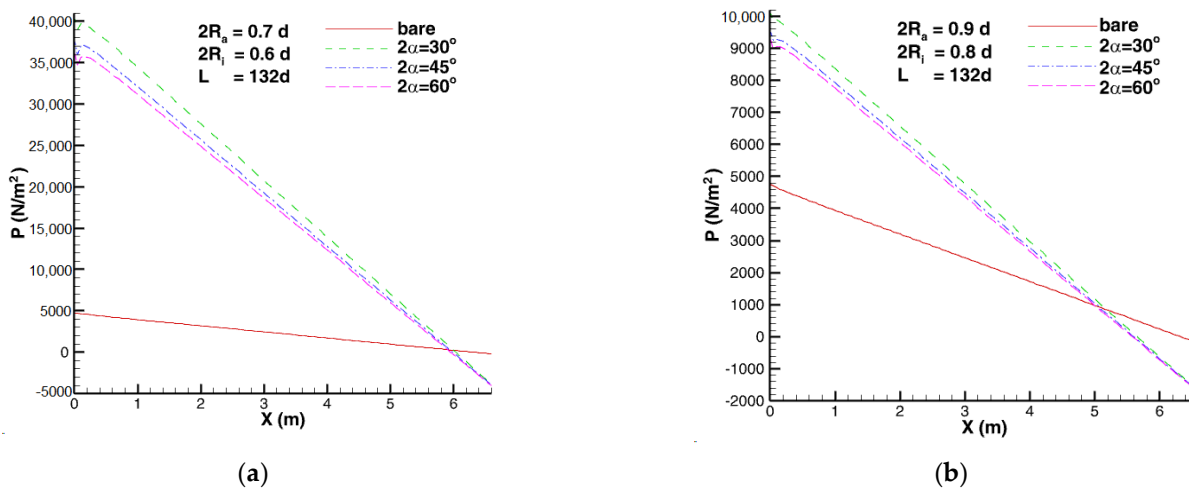


Figure 6. Variation of the cross-sectional average pressure: (a) $2Ra = 0.7d$, $2Ri = 0.6d$, $L = 132d$; (b) $2Ra = 0.9d$, $2Ri = 0.8d$, $L = 132d$.

The effect of the fin angle on the cross-sectional average temperature along the tube is shown in Figure 7. A larger fin angle yields a lower temperature. This is because a larger fin angle corresponds to fewer fins, which in turn have a smaller inner surface area and lower frictional heating effect.

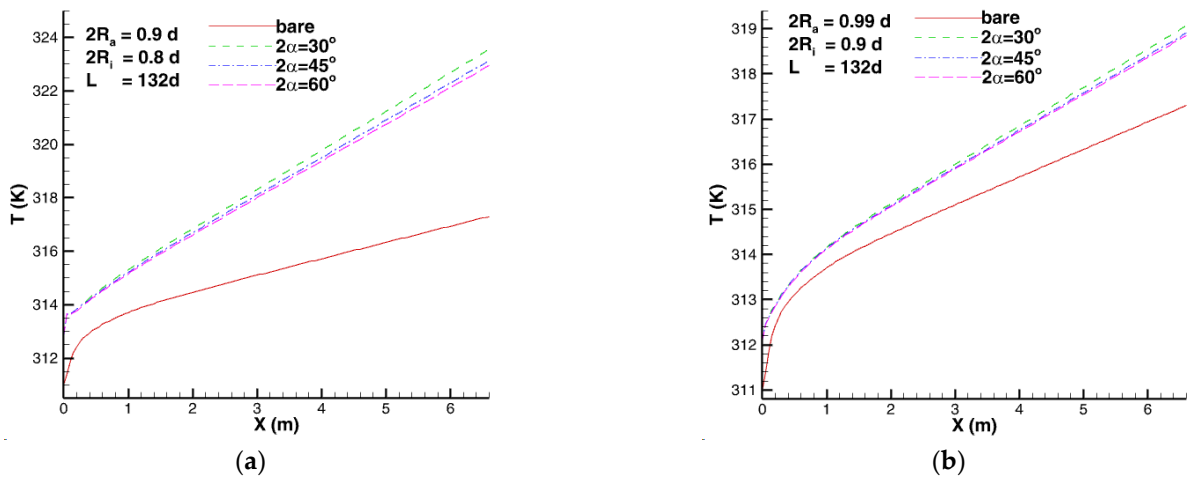


Figure 7. Variation of the cross-sectional average temperature: (a) $2R_a = 0.9d$, $2R_i = 0.8d$, $L = 132d$; (b) $2R_a = 0.99d$, $2R_i = 0.9d$, $L = 132d$.

The effect of the fin angle on the temperature uniformity index along the tube is shown in Figure 8. Compared to a bare tube, SIFT improves its temperature uniformity. However, the influence of the fin angle on the temperature uniformity is not significant, although a careful observation reveals that a larger fin angle yields better uniformity. This is because more fins (smaller fin angles) result in faster flow acceleration in the fin region and alleviates the secondary flow (Dean Vortex) at the cross-section, which leads to worse mixing. The smaller the fin angle is, the worse the temperature uniformity will be.

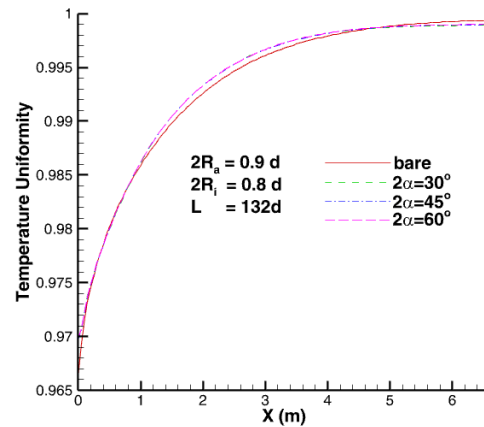


Figure 8. Temperature uniformity index along the tube.

The effect of fin amplitude on the pressure variation along the tube is shown in Figure 9. It can be seen that a larger contraction, i.e., a smaller R_a for a given R_i or a smaller R_i for a given R_a , yields a larger pressure drop. This is because a larger contraction results in a higher flow velocity, and therefore, the pressure drop is higher.

The effect of fin amplitude on the cross-sectional average temperature distribution is shown in Figure 10. The fin amplitude has an obvious influence on the temperature variation. A larger contraction, i.e., a smaller R_i for a given R_a , yields a higher temperature. This is because a larger contraction results in a higher flow velocity. Therefore, the temperature increases due to the higher wall friction.

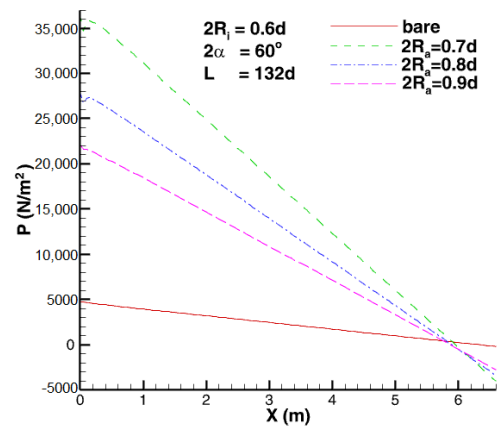


Figure 9. Variation of the cross-sectional average pressure.

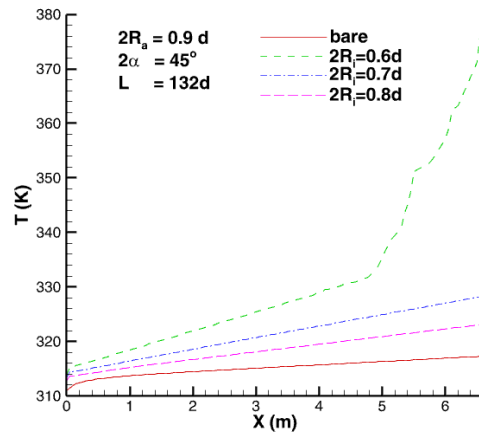


Figure 10. Variation of the cross-sectional average temperature.

The effect of the fin amplitude on the temperature uniformity index is shown in Figure 11. SIFT improves the temperature uniformity index for a smaller fin amplitude, i.e., a smaller $2(R_a - R_i)$, as compared to a bare tube. This is because a larger fin amplitude may alleviate the secondary flow (Dean Vortex) at the cross-section because of a higher flow acceleration, which leads to worse mixing. The larger the fin amplitude is, the worse the temperature uniformity will be.

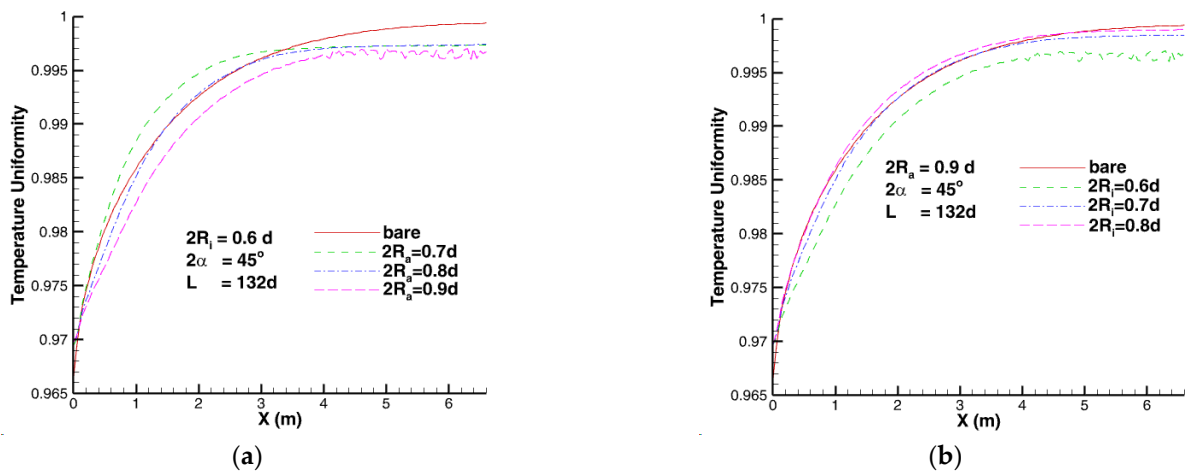


Figure 11. Temperature uniformity index along the tube: (a) $2R_i = 0.6d$, $2\alpha = 45^\circ$, $L = 132d$; (b) $2R_a = 0.9d$, $2\alpha = 45^\circ$, $L = 132d$.

4. Conclusions

The performance of the SIFT concerning the heat transfer enhancement and the pressure drop was investigated using CFD to obtain optimal temperature uniformity and reduce pressure drop. A longer fin yields a larger pressure drop, which is nearly proportional to the fin length. When the fin length is larger than 30 d, the pressure drop becomes greater than that of a bare tube. The temperature of the SIFT is higher than that of a bare tube. The temperature increases with the fin length, rises abruptly at the fin inlet, and descends abruptly at the fin outlet. The SIFT improves the temperature uniformity compared to a bare tube. However, there is no need to use an SIFT with a long fin. A fin length of 10 d is enough to obtain satisfactory temperature uniformity. A smaller fin angle yields a larger pressure drop. The temperature decreases with the fin angle. A larger fin angle yields better temperature uniformity. A larger contraction yields a larger pressure drop and a higher temperature rise. Finally, the temperature uniformity is improved by the SIFT for a smaller fin amplitude.

Author Contributions: Conceptualization, C.-L.Y.; methodology, C.-L.Y.; validation, C.-L.Y.; formal analysis, C.-L.Y.; data curation, C.-L.Y., D.-L.W., Q.-Y.C., Y.-X.C., C.-X.L. and Z.-Q.W.; writing—original draft preparation, C.-L.Y.; writing—review and editing, C.-L.Y., D.-L.W., Q.-Y.C., Y.-X.C., C.-X.L. and Z.-Q.W.; visualization, C.-L.Y., D.-L.W., Q.-Y.C., Y.-X.C., C.-X.L. and Z.-Q.W. All authors have read and agreed to the published version of the manuscript.

Funding: This research received no external funding.

Institutional Review Board Statement: Not applicable.

Informed Consent Statement: Not applicable.

Data Availability Statement: The data presented in this study are available on request from the corresponding author.

Conflicts of Interest: The authors declare no conflict of interest.

References

1. Albano, J.; Rhoe, A.; Sundaram, K.; Summer, C. Pyrolysis Heater. European Patent 0,305,799, B1, 23 October 1991.
2. Albano, J.; Sundaram, K.; Maddock, M. Application of extended surface in pyrolysis coils. *Eng. Prog.* **1988**, *8*, 160–168.
3. Brown, D. Internally finned radiant coils: A valuable tool for improving ethylene plant economics. In Proceedings of the 6th EMEA Petrochemicals Technology Conference, London, UK, 23–26 June 2004.
4. Schietekat, C.M.; Cauwenberge, D.V.; Geem, K.V.; Marin, G.B. Computational fluid dynamics based design of finned steam cracking reactors. In Proceedings of the AIChE Spring Meeting: Ethylene Producers Conference—Fundamentals of Technology Session, San Antonio, TX, USA, 2 May 2013.
5. Wölpert, P.; Ganser, B.; Jakobi, D.; Kirchheiner, R. Finned Tube for the Thermal Cracking of Hydrocarbons, and Process for Producing a Finned Tube. U.S. Patent 7,963,318 B2, 21 June 2011.
6. Yeh, C.L.; Wu, D.L.; Cai, Q.Y.; Yang, S.Y.; Lin, X.J.; Liu, G.H. Parametric study on the performance of a helical type of internally finned tube. In Proceedings of the 2022 IEEE 4th Eurasia Conference on IOT, Communication and Engineering, Yunlin, Taiwan, 28–30 October 2022.
7. Fluent Inc. *ANSYS FLUENT 17 User's Guide*; Fluent Inc.: New York, NY, USA, 2017.
8. Patankar, S.V. *Numerical Heat Transfer and Fluid Flows*; McGraw-Hill: New York, NY, USA, 1980.
9. Siegel, R.; Howell, J.R. *Thermal Radiation Heat Transfer*; Hemisphere Publishing Corporation: Washington, DC, USA, 1992.

Disclaimer/Publisher's Note: The statements, opinions and data contained in all publications are solely those of the individual author(s) and contributor(s) and not of MDPI and/or the editor(s). MDPI and/or the editor(s) disclaim responsibility for any injury to people or property resulting from any ideas, methods, instructions or products referred to in the content.